Research Square

Preprints are preliminary reports that have not undergone peer review.
They should not be considered conclusive, used to inform clinical practice,
or referenced by the media as validated information.

Fasting Plasma Glucose and Alanine Aminotransferase Levels in Adults Aged 45–65 Years With Elevated ALT: A Cross-Sectional Study

Zhengyu Chen
The Second Hospital of Nanjing
Xiaoyu Zhang
zhangxiaoyu02@sina.com
The Second Hospital of Nanjing
Lili Huang
The Second Hospital of Nanjing

Research Article

Keywords: metabolic dysfunction-associated steatotic liver disease, fasting plasma glucose, alanine aminotransferase, liver injury, insulin resistance, FIB-4, lactylation

Posted Date: November 16th, 2026

DOI: https://doi.org/10.21203/rs.3.rs-11180844/v1

License: This work is licensed under a Creative Commons Attribution 4.0 International License.
Read Full License

Additional Declarations: No competing interests reported.

Fasting Plasma Glucose and Alanine Aminotransferase Levels in Adults Aged 45 – 65 Years With Elevated ALT: A Cross-Sectional Study

Zhengyu Chen[a],Xiaoyu Zhang[a*], Lili Huang[a]

a. Department of Infectious Disease and Liver Disease, The Second Hospital of Nanjing (Nanjing, 210000), China

*Correspondence:zhangxiaoyu02@sina.com

Abstract

Background. Metabolic dysfunction-associated steatotic liver disease (MASLD) is a leading cause of chronic liver injury, and both excess adiposity and dysglycaemia have been implicated in its progression. However, the association between fasting plasma glucose and ALT after accounting for adiposity remains insufficiently characterised in adults aged 45–65 years presenting with elevated ALT.

Methods. We conducted a cross-sectional study of 511 adults aged 45–65 years with elevated serum alanine aminotransferase (ALT) attending a metabolic liver clinic. Participants were stratified by fasting plasma glucose (FPG) into four groups: normal (<5.6 mmol/L), impaired fasting glucose (5.6 to <7.0), diabetic range (7.0 to <10.0) and markedly elevated (≥10.0). The primary outcome was ALT analysed as log-transformed continuous values; secondary outcomes were marked ALT elevation (ALT ≥3× upper limit of normal [ULN]) and elevated FIB-4 (≥2.67). Multivariable linear and logistic regression adjusted for sex, age, body mass index (BMI), waist circumference, triglycerides, total cholesterol and uric acid. Exploratory liver transcriptomic analyses of glycolysis, insulin-signalling and lactylation-related gene sets were performed in three public cohorts.

Results. Higher fasting glucose was associated with higher ALT levels in a graded manner. After adjustment, ALT was 1.28-fold (95% CI 1.07–1.52), 1.66-fold (1.36–2.02) and 2.68-fold (2.06–3.47) higher in the impaired-fasting-glucose, diabetic-range and markedly-elevated groups than in the normal group; each 1 mmol/L increment in fasting glucose was associated with a 9.0% increase in ALT (geometric mean ratio 1.09, 95% CI 1.06–1.12; $P = 2.4\times10^{-19}$). The association persisted in participants with imaging-confirmed steatosis (GMR 1.089), and a parallel analysis using HbA1c gave a similar estimate (13.5% higher ALT per 1-percentage-point increment; $P = 9.5\times10^{-11}$). The association was directionally consistent across subgroups, although effect size differed across some strata. Glycaemic control was poor: only 3.3% of participants with diabetes had fasting glucose below 7.0 mmol/L. Exploratory liver transcriptomic analyses identified glycolysis- and lactylation-related signatures associated with serum ALT; no statistically significant association of module scores with fasting glucose or HOMA-IR was detected. These transcriptomic findings are hypothesis-generating.

Conclusions. Among adults aged 45–65 years referred for elevated ALT, higher fasting plasma glucose was associated with higher ALT levels after adjustment for measured adiposity and other metabolic factors, and glycaemic control was markedly suboptimal in this population (median HbA1c 9.4% among participants with previously diagnosed diabetes). Exploratory liver transcriptomic analyses identified related metabolic signatures associated with hepatic injury. These cross-sectional findings do not establish causality and warrant longitudinal validation.

Keywords: metabolic dysfunction-associated steatotic liver disease; fasting plasma glucose; alanine aminotransferase; liver injury; insulin resistance; FIB-4; lactylation

1. Introduction

Chronic liver disease related to metabolic dysfunction has become the most rapidly growing indication for liver transplantation and a major contributor to liver-related morbidity worldwide [1]. The 2023 nomenclature revision introduced metabolic dysfunction-associated steatotic liver disease (MASLD) to emphasise the causal role of cardiometabolic risk factors, and established that the disease spans a spectrum from isolated steatosis through steatohepatitis to progressive fibrosis and cirrhosis [2]. Elevated aminotransferases remain the most frequent trigger for clinical referral, yet the severity of enzyme elevation varies widely among patients carrying apparently similar metabolic risk profiles.

Obesity has traditionally been regarded as the dominant driver, and body mass index (BMI) remains the most widely used triage parameter in clinical practice. However, a substantial proportion of patients with steatotic liver disease are not obese, and conversely many individuals with obesity maintain normal aminotransferases. This discordance indicates that other cardiometabolic exposures may also contribute. Among these, dysglycaemia is mechanistically attractive: insulin resistance has been reported to increase hepatic de novo lipogenesis and oxidative stress and to promote intracellular lactate accumulation [3]; in experimental models, lactate-derived histone lysine lactylation has been linked to pro-inflammatory and pro-fibrotic transcriptional programmes [4].

Despite this biological plausibility, the relative contribution of glucose status versus adiposity to ALT levels has rarely been quantified in a directly comparative manner. Most previous studies have examined either obesity or diabetes in isolation, adjusted for the other only superficially, or were conducted in general-population samples in which enzyme elevation was uncommon. Middle-aged and older adults, the group at highest fibrosis risk [5], have also been under-represented in cohorts recruited from younger referral populations.

We therefore assembled a cohort of 511 adults aged 45–65 years presenting with elevated ALT and evaluated the association between fasting plasma glucose (FPG) and ALT levels after adjustment for adiposity and other cardiometabolic parameters. We additionally assessed glycaemic control in the subgroup with previously diagnosed diabetes and performed exploratory

transcriptomic analyses in public MASLD cohorts to provide context for liver disease–associated transcriptional changes.

2. Materials and methods

2.1 Study design and participants

This was a single-centre, cross-sectional study conducted at The Second Hospital of Nanjing between January 2021 and June 2026. Consecutive adults aged 45–65 years referred for evaluation of elevated serum alanine aminotransferase (ALT) were screened for eligibility. Inclusion criteria were: (i) age 45–65 years; (ii) serum ALT above the upper limit of normal on at least two occasions; and (iii) availability of a complete fasting metabolic panel. Exclusion criteria were: positive hepatitis B surface antigen or anti-hepatitis C virus antibody; self-reported alcohol consumption ≥140 g/week (men) or ≥70 g/week (women); other known chronic liver disease; chronic kidney disease stage ≥3; and current use of hepatotoxic medication. This study adopted a retrospective design, and therefore ethical approval was exempted. The participant selection process is summarised in Figure 1a.

2.2 Clinical and laboratory assessment

Anthropometric measurements, including height, weight, waist circumference and blood pressure, were obtained by trained personnel using standardised procedures. Handgrip strength was measured with a digital dynamometer. Venous blood was collected after an overnight fast of at least 8 hours. Biochemical parameters included ALT, aspartate aminotransferase (AST), γ-glutamyl transferase, alkaline phosphatase, total bilirubin, albumin, total cholesterol, triglycerides, high-density lipoprotein cholesterol, low-density lipoprotein cholesterol, fasting plasma glucose, glycated haemoglobin (HbA1c), uric acid and creatinine. A complete blood count was performed to obtain platelet count. Serum lactate was measured under standardised resting conditions. Biochemical assays were performed on a standardised automated clinical chemistry platform using IFCC-aligned methods at 37 °C. Ultrasonography, transient elastography and venous blood collection were performed on the same day, and imaging data were available for all participants. Hepatic steatosis was assessed by abdominal ultrasonography and graded semi-quantitatively (0–3) on standardised criteria (hepatorenal echogenicity contrast, deep beam attenuation and vascular blurring) [6]; the controlled attenuation parameter (CAP, dB/m) was recorded as an auxiliary quantitative measure [7]. MRI-PDFF and liver biopsy were not performed in this cohort; the steatosis component of the MASLD definition was therefore based on ultrasound. Liver stiffness was measured by transient elastography with at least 10 valid acquisitions and an interquartile-range/median ratio below 30% [7,8]; stiffness ≥8 kPa was considered suggestive of clinically significant fibrosis [8]. For fibrosis risk stratification, FIB-4 was categorised as low (<1.3), indeterminate (1.3–2.67) and high (≥2.67) risk and interpreted together with liver stiffness [9].

2.3 Definitions and outcomes

Fasting glucose status was categorised according to American Diabetes Association criteria [10] as: normal (<5.6 mmol/L), impaired fasting glucose (5.6 to <7.0 mmol/L), diabetic range (7.0 to <10.0 mmol/L) and markedly elevated (≥10.0 mmol/L). Glucose categories were defined for analytical purposes and were not intended to establish a clinical diagnosis of diabetes from a single fasting glucose measurement. The primary outcome was serum ALT, analysed after natural logarithmic transformation because of its right-skewed distribution; a value of 120 U/L corresponds to three times the laboratory upper limit of normal (ULN, 40 U/L, identical for men and women in this cohort), and values above this ULN constituted the elevated-ALT inclusion criterion. Secondary outcomes were marked ALT elevation (ALT ≥3×ULN, ≥120 U/L) and elevated FIB-4 (≥2.67). ALT ≥5×ULN (≥200 U/L) was evaluated as an exploratory outcome. Elevated FIB-4 was likewise retained as an exploratory secondary outcome because FIB-4 is derived from aminotransferases and enrolment was based on elevated ALT, so elevated FIB-4 should not be equated with confirmed structural fibrosis. FIB-4 was calculated as [age × AST] / [platelet count × √ALT] [9]; the NAFLD fibrosis score (NFS) [11] and APRI [12] were calculated as prespecified indices of fibrosis risk. Metabolic dysfunction was defined according to the MASLD criteria of the 2023 consensus statement [2]. The primary analysis included all participants meeting the ALT-elevation inclusion criterion; an additional sensitivity analysis was restricted to participants with imaging-confirmed hepatic steatosis who additionally met the 2023 MASLD criteria (steatosis plus at least one cardiometabolic risk factor). Because enrolment was based on elevated ALT rather than imaging-defined steatosis, the cohort is described as an elevated-ALT population, of whom a substantial subset met the MASLD definition, rather than as a uniformly MASLD cohort.

2.4 Statistical analysis

Continuous variables are presented as mean ± standard deviation or median (interquartile range) according to distribution, and categorical variables as counts (percentages). Between-group comparisons used one-way ANOVA or Kruskal–Wallis tests, and trend across glucose strata was assessed by linear regression with fasting glucose as a continuous predictor. Multivariable linear regression on log-transformed ALT and logistic regression for secondary outcomes were fitted in three hierarchically adjusted models: Model 1 unadjusted; Model 2 adjusted for age and sex; and Model 3 additionally adjusted for BMI, waist circumference, triglycerides, total cholesterol and uric acid. Because the log-transformed ALT model was linear, exponentiated coefficients are reported as geometric mean ratios (GMR). The primary analysis was the association of continuous fasting glucose with log-transformed ALT; restricted cubic splines characterised the dose–response shape; and stratum-specific GMRs relative to the normal group provided a categorical display. Additional sensitivity analyses included alternative adiposity adjustment (BMI alone or waist circumference alone), a parallel analysis using HbA1c as the exposure, and restriction to participants meeting the MASLD definition. Restricted cubic splines with four knots (placed at the 5th, 35th, 65th and 95th percentiles of fasting glucose: 4.3, 6.05, 8.3 and 17.95 mmol/L) were used to examine non-linearity [13], with overall and non-linear associations tested by likelihood-ratio nested comparisons. For discrimination analyses, the base clinical model

comprised age, sex, BMI, waist circumference, triglycerides, total cholesterol and uric acid, and fasting-glucose strata were then added; discrimination was quantified as the apparent (in-sample) area under the receiver-operating-characteristic curve for marked ALT elevation, with bootstrap 95% confidence intervals from 1,000 resamples and between-model comparison with the DeLong test [14]. No external validation or optimism correction was performed. Prespecified subgroup analyses used multiplicative interaction terms. Exploratory piecewise models used a clinically motivated breakpoint at 7.0 mmol/L (the ADA diagnostic threshold [10]). All analysed variables were complete for the 511 included participants, so no imputation was required and all analyses were complete-case. Collinearity among covariates was assessed with variance inflation factors (VIF), values above 10 being considered indicative of problematic collinearity. For the transcriptomic analyses, P values were adjusted within each gene-set library and contrast using the Benjamini–Hochberg false discovery rate (FDR) [15]; nominal P values are reported where indicated. Exploratory subgroup, piecewise and secondary-outcome analyses were not adjusted for multiplicity and are interpreted accordingly. Analyses were performed in Python 3.13 (statsmodels 0.14); two-sided $P < 0.05$ was considered significant. Reporting follows the STROBE statement for cross-sectional studies [16]; the completed checklist is provided as supplementary material.

2.5 Exploratory liver transcriptomic analyses

Three publicly available human liver transcriptomic datasets were obtained from GEO: GSE48452 (Affymetrix HG-1.1-ST arrays; 18 NASH vs 14 healthy controls) [17], GSE89632 (Illumina HT-12 arrays; 19 NASH vs 24 healthy donors, with per-sample fasting glucose, HOMA-IR and ALT) [18] and GSE135251 (RNA-seq of 216 liver biopsies spanning fibrosis stages F0–4) [19]. Raw GSE135251 counts were filtered (CPM > 1 in ≥25% of samples), normalised to log2(CPM + 1), and identifiers were mapped to HGNC symbols (highest-mean probe retained per symbol; array platforms re-annotated from GPL records). Differential expression was tested with an empirical-Bayes moderated t-statistic.

Gene-set enrichment used GSEA in preranked mode [20] against four libraries (MSigDB Hallmark [21], KEGG [22], Reactome [23] and a custom set collection covering the lactylation machinery, glycolysis/lactate metabolism and insulin signalling; 1,000 gene permutations), tested against both binary contrasts and continuous phenotypes (NAFLD activity score and fibrosis stage). Single-sample module scores were computed as the mean per-sample z-score of detected genes within each custom set. Immune deconvolution used 16 marker-based cell-type signatures [24], scored with a single-sample gene-set enrichment scoring (ssGSEA-type) approach [25]. Module–trait associations were examined with Spearman correlation and, as a check, with rank-based partial Spearman correlation adjusting for age, sex and BMI; associations were computed both in all samples and within cases separately to distinguish case–control differences from within-disease gradients. Module–trait associations are reported per trait without combination into pooled statistics, because the different phenotypes do not represent a single estimand and the within-sample test statistics are correlated. All analyses were performed in Python (pandas, statsmodels, scipy, gseapy [26]).

For each dataset, sample selection, inclusion criteria, clinical phenotyping and assay procedures were as described in the original publications (GSE48452, GSE89632 and GSE135251) [17–19]. The three datasets were analysed independently without cross-dataset integration, so no between-dataset batch-effect correction was required; preprocessing within each dataset was as described above. Immune and stromal cell-type scores were computed with a marker-based single-sample gene-set scoring approach: for each of 16 curated signatures, the per-sample score was the mean of the z-scored expression of its marker genes (z-scores computed across samples within each dataset). The three custom gene sets (lactylation machinery, glycolysis/lactate metabolism and insulin signalling) were assembled from curated pathway members and are listed in full in Supplementary Table S2. Enrichment P values were adjusted by the Benjamini–Hochberg FDR within each gene-set library and contrast.

3. Results

3.1 Baseline characteristics

A total of 511 participants were included (301 men [58.9%]; median age 55 years, interquartile range 51–59). Overall, 210 participants (41.1%) had previously diagnosed diabetes recorded in the medical record. Stratification by fasting glucose status yielded 132 participants (25.8%) in the normal group, 123 (24.1%) with impaired fasting glucose, 111 (21.7%) in the diabetic range and 145 (28.4%) with markedly elevated glucose. Cardiometabolic burden increased monotonically across strata: BMI rose from 23.4±0.9 to 28.2±1.6 kg/m², waist circumference from 80.0±4.9 to 93.1±7.3 cm, triglycerides from 2.0±0.8 to 3.0±0.6 mmol/L and HbA1c from 4.91±0.42% to 10.53±1.89% (all P for trend <0.001). Median ALT increased progressively from 128 (78–181) U/L in the normal group to 192 (140–247) U/L in the markedly elevated group, and median AST from 46 (30–86) to 95 (70–135) U/L (both P for trend <0.001). Serum lactate also increased monotonically (1.20±0.29 to 1.77±0.35 mmol/L; P for trend <0.001), as did median FIB-4 (1.35 to 1.86; $P = 3.8\times10^{-8}$) and the prevalence of elevated FIB-4 (7.6% to 26.2%). By contrast, γ-glutamyl transferase, platelet count and albumin did not differ across glucose strata (all P > 0.05) (Table 1). Hepatic steatosis on ultrasound was present in 385 participants (75.3%), with moderate-to-severe steatosis (grade 2–3) in 218 (42.7%); the prevalence rose from 39.4% in the normal-glucose group to 96.6% in the markedly-elevated group. The remaining 126 participants (24.7%) had no imaging evidence of steatosis despite persistently elevated ALT; imaging data were available for all 511 participants. Median liver stiffness was 5.3 kPa (IQR 4.6–6.2), and only 3.1% had stiffness ≥8 kPa (Table 5) (Figure 1).

3.2 Dose–response association between fasting glucose and ALT levels

In the linear model on log-transformed ALT (Model 3), relative to the normal group, ALT was 1.28-fold higher (95% CI 1.07–1.52; P = 0.006) in the impaired-fasting-glucose group, 1.66-fold higher (1.36–2.02; $P = 7.5\times10^{-7}$) in the diabetic-range group and 2.68-fold higher (2.06–3.47; $P = 4.5\times10^{-13}$) in the markedly-elevated group (Figure 2A, Supplementary Table S1). Treated as a

continuous variable, each 1 mmol/L increment in fasting glucose was associated with a 9.0% increase in ALT (geometric mean ratio 1.090, 95% CI 1.062–1.118; $P = 2.4\times10^{-10}$) (Figure 2B). Restricted cubic spline analysis with four knots showed a significant overall association (P-overall = 1.1×10^{-16}) with evidence of non-linearity (P-nonlinear = 8.0×10^{-9}): the slope was steeper below approximately 7.0 mmol/L and flatter above (Figure 2). An exploratory piecewise linear model with a clinically motivated breakpoint at 7.0 mmol/L (the ADA diagnostic threshold) estimated an ALT fold change per mmol/L of ×1.372 below 7.0 versus ×1.095 above (slope-change $P < 0.0001$). The piecewise model is reported as a descriptive complement to the spline and does not imply a biological threshold.

3.3 Glucose status and categorical liver outcomes

The prevalence of marked ALT elevation (ALT ≥3×ULN) rose from 53.8% in the normal group to 83.4% in the markedly-elevated group. ALT ≥5×ULN, analysed as an exploratory outcome, rose from 17.4% to 46.9%. In logistic regression adjusted as in Model 3, each 1 mmol/L increment in fasting glucose was associated with an odds ratio of 1.211 (95% CI 1.099–1.335; $P = 1.1\times10^{-4}$) for ALT ≥3×ULN and 1.175 (1.067–1.294; $P = 1.0\times10^{-3}$) for ALT ≥5×ULN. For elevated FIB-4 (≥2.67), retained as an exploratory secondary outcome, the adjusted odds ratio was 1.274 (1.103–1.471; $P = 9.6\times10^{-4}$) (Table 2). Adding glucose strata to the base clinical model was associated with a modest increase in apparent (in-sample) discrimination of marked ALT elevation (AUC 0.605 to 0.674; ΔAUC +0.069, bootstrap 95% CI 0.020–0.120; DeLong P = 0.006; ΔAIC −29.4) (Figure 4).

3.4 Association after adjustment for adiposity and other metabolic factors

The association between fasting glucose and ALT remained statistically significant after adjustment for measured adiposity and other metabolic covariates; the increase in the adjusted effect estimate relative to the unadjusted estimate was examined in the collinearity and sensitivity analyses of Section 3.4b. Each 1 mmol/L increment in fasting glucose was associated with a geometric mean ratio of ALT of 1.050 (95% CI 1.037–1.063) unadjusted, 1.051 (1.038–1.065) after adjustment for age and sex, and 1.090 (1.062–1.118; $P = 2.4\times10^{-10}$) after additional adjustment for BMI, waist circumference, triglycerides, total cholesterol and uric acid (Model 3); covariate estimates are given in Table 3, and collinearity diagnostics in Section 3.4b. Adding glucose strata to the clinical model increased the explained variance in ALT from $R^2 = 0.063$ to $R^2 = 0.168$ ($\Delta R^2 = 0.104$; nested-model $F = 20.8$, $P = 9.7\times10^{-13}$). The corresponding improvement in discrimination of elevated FIB-4 was modest and not significant (ΔAUC +0.029, bootstrap 95% CI −0.002 to +0.059; DeLong P = 0.072).

3.4b Stability of the glucose–ALT association

Additional sensitivity analyses assessed the stability of the estimate. Spearman correlations among continuous covariates are given in Supplementary Table S3. Antihyperglycaemic medication use was not included as a model covariate because it is strongly collinear with prior diabetes diagnosis and lies downstream of long-term glycaemia; medication use is reported

descriptively (Tables 4 and 5). First, in a parallel model using HbA1c as the exposure, each 1-percentage-point increment in HbA1c was associated with a 13.5% increase in ALT (geometric mean ratio 1.135, 95% CI 1.093–1.179; $P = 9.5\times10^{-11}$), in agreement with the fasting-glucose result. Second, restricting the analysis to the 385 participants with imaging-confirmed steatosis who met the MASLD definition, each 1 mmol/L increment in fasting glucose was associated with an 8.9% increase in ALT (GMR 1.089, 95% CI 1.059–1.120; $P = 7.1\times10^{-9}$), essentially identical to the estimate in the full cohort (1.090, 1.062–1.118). Third, the fasting-glucose estimate was stable across adiposity adjustment strategies: GMR 1.087 when BMI was included without waist circumference (Model 3a), 1.086 with waist circumference without BMI (Model 3b), and 1.090 with both (Model 3c). Variance inflation factors in the fully adjusted model were 1.0 for age, 8.2 for male sex, 4.4 for fasting glucose, 11.9 for BMI, 19.3 for waist circumference, 1.3 for triglycerides, 1.6 for total cholesterol and 2.4 for uric acid; only the adiposity pair exceeded the conventional threshold of 10, and estimates are therefore reported for the model including both for consistency. Fourth, the association persisted after excluding the 177 participants using antihyperglycaemic medication (n = 334; GMR 1.124, 95% CI 1.076–1.173; $P = 2.5\times10^{-7}$) and after excluding extreme values (ALT >1000 U/L or fasting glucose >20 mmol/L; n = 497; GMR 1.106, 95% CI 1.077–1.137; $P = 1.0\times10^{-12}$). In participants without a recorded diabetes diagnosis (n = 301), the association was imprecisely estimated (GMR 0.882, 95% CI 0.502–1.548); the fasting-glucose range was restricted in this subgroup because all 53 participants with diabetic-range glucose were newly identified, limiting within-group exposure contrast.

Liver stiffness and FIB-4 showed limited concordance: of 80 participants with FIB-4 ≥2.67, only 6 also had liver stiffness ≥8 kPa, whereas 10 of 431 with FIB-4 <2.67 had stiffness ≥8 kPa. Because FIB-4 is derived from aminotransferases and enrolment was based on elevated ALT, elevated FIB-4 in this population should not be equated with confirmed structural fibrosis; conversely, liver stiffness is itself influenced by inflammatory activity and is not an absolute gold standard. Elevated FIB-4 is therefore retained as an exploratory secondary outcome, and no binary stiffness analysis was performed given the small number of events (16 participants with stiffness ≥8 kPa).

3.5 Subgroup analyses

The association was directionally consistent across all prespecified subgroups when expressed per 1 mmol/L increment in fasting glucose. The adjusted GMR was stronger in the lowest BMI tertile (1.19 versus 1.11 in the highest; interaction P = 0.003), in participants without central obesity (1.16 versus 1.11; interaction P < 0.001), in those with mild or no steatosis on ultrasound (1.16 versus 1.08; interaction P < 0.001), and in those with FIB-4 <1.3 (1.15 versus 1.00; interaction P = 0.005). Associations by sex and by triglyceride level (TG ≥1.7 vs <1.7 mmol/L) did not differ significantly. These interaction tests indicate heterogeneity in effect size across some subgroups, and are exploratory. When participants were instead stratified by previously diagnosed diabetes, within-stratum estimates were imprecise: only 7 of 210 participants with diabetes had fasting glucose below 7.0 mmol/L at the study visit, so the exposure range within the diabetes stratum

was restricted and a reliable interaction test could not be performed; these estimates are shown in Figure 3 without an interaction test.

3.6 Suboptimal glycaemic control and under-recognition of dysglycaemia

Among 210 participants with a recorded diagnosis of diabetes, only 7 (3.3%) had fasting glucose below 7.0 mmol/L at the study visit, and the median HbA1c was 9.4% (IQR 7.5–11.1), with 174 of 210 (82.9%) at or above 7.0%. Median diabetes duration was 10.4 years. Antihyperglycaemic treatment was documented in 172 of 210 (81.9%) participants with diabetes (metformin 102, sulphonylureas 26, insulin 21, metformin plus other agents 15, GLP-1 receptor agonists 8); cohort-wide, 177 participants used antihyperglycaemic medication, the five additional users having no recorded diabetes diagnosis (Table 5). In the cohort as a whole, 256 participants (50.1%) had fasting glucose ≥7.0 mmol/L, of whom 53 had no recorded diabetes diagnosis; among the latter, confirmatory testing would be required to establish a diagnosis. Within the subgroup with previously diagnosed diabetes, differences in ALT across current fasting-glucose categories were imprecisely estimated; restricted exposure range, treatment effects and limited subgroup size may have contributed to these findings (Table 4, Table 5).

3.7 Exploratory transcriptomic analyses in three public MASLD cohorts

Glycolysis showed consistent positive enrichment in NASH across cohorts and across contrast definitions: KEGG glycolysis/gluconeogenesis NES = +2.08 (FDR = 0.001) in GSE48452 and NES = +1.64 (FDR = 0.033) in GSE89632, and NES = +1.4 against continuous NAFLD activity score in GSE135251 (nominal P = 0.007–0.012). The custom insulin-signalling signature was significantly enriched in NASH in GSE89632 (NES = +1.52, P = 0.017, FDR = 0.014), and its single-sample score correlated with serum ALT (Spearman $\rho = 0.43$, P = 0.0005); this association survived adjustment for age, sex and BMI (partial $\rho = 0.36$, P = 0.006). The lactylation machinery score likewise correlated with ALT ($\rho = 0.33$, P = 0.009; partial $\rho = 0.28$, P = 0.029), and the combined glycolysis/lactate score correlated with histological activity ($\rho = 0.39$, P = 0.009; partial $\rho = 0.31$, P = 0.043) (Figure 5).

In GSE135251, insulin-signalling enrichment was strongly negative with respect to both continuous fibrosis stage (NES = −1.7, nominal P < 0.001) and binary advanced fibrosis (F3–4 vs F0–1; NES = −1.6), whereas the glycolysis and lactylation sets remained positive against disease activity. This stage-dependent dissociation, with enrichment in inflammatory steatotic disease but depletion in advanced fibrosis, is consistent with metabolic dedifferentiation of hepatocytes as fibrosis progresses, and cautions against interpreting the insulin-signalling signal as a monotonic marker of disease severity. Marker-based immune deconvolution in GSE135251 identified fibroblast activation as the dominant stromal signal ($\rho = 0.51$ with fibrosis stage, $P < 10^{-4}$), accompanied by increases in plasma cells, dendritic cells, mast cells and M1-polarised macrophages (Figure 6A, B).

3.8 Stability of the module–trait associations

Because insulin-signalling enrichment changed direction across contrast definitions, GSEA was repeated against continuous phenotypes. All glycolysis-related and lactylation sets retained positive enrichment against continuous NAFLD activity score, indicating that the glycolytic signal is not an artefact of binary contrast choice. Rank-based partial Spearman analysis adjusting for age, sex and BMI did not attenuate the module–liver-injury associations, which were also present when computed within cases separately. In contrast, no module score was significantly associated with fasting glucose (n = 57; Spearman ρ +0.04 to +0.19, all 95% confidence intervals crossing zero) or HOMA-IR (n = 49; ρ −0.02 to +0.25, all intervals crossing zero); the intervals were wide and remain compatible with weak-to-moderate associations, so these null findings do not exclude a relationship with systemic glycaemia. These exploratory findings provide context for liver disease–associated transcriptional changes but do not establish a mechanistic link between systemic glycaemia and hepatic injury (Figure 6C, D). The lactylation-related gene sets capture coordinated expression of lactylation-machinery genes and do not directly measure protein or histone lactylation levels.

4. Discussion

In this cross-sectional study of 511 adults aged 45–65 years referred for elevated ALT, higher fasting plasma glucose was associated with higher ALT levels. The association was dose-dependent, persisted after adjustment for adiposity, lipid indices and uric acid, and was directionally consistent across subgroups. Adding glucose to a clinical model increased the explained variance in ALT and the discrimination of marked ALT elevation. These findings suggest that glycaemic assessment deserves a prominent place alongside anthropometry in the evaluation of patients presenting with elevated ALT. Because inclusion was conditional on elevated ALT, the observed associations may not represent those in an unselected population; selection on an outcome influenced by multiple metabolic factors may also distort their relative associations. Accordingly, the lack of statistical significance for adiposity measures should not be interpreted as evidence that adiposity is unimportant in liver disease.

That the glucose–ALT association strengthened after adjustment for adiposity runs counter to the usual pattern: obesity and dysglycaemia are strongly correlated, and adjustment tends to attenuate associations. One explanation is collinearity: in this cohort BMI and fasting glucose were closely related, and the BMI coefficient in the adjusted model may therefore be unstable. A complementary interpretation is that adipose tissue expansion and hyperglycaemia contribute to liver injury through partially distinct pathways, with insulin resistance and hepatic substrate overload acting downstream of, or in parallel to, adiposity. This is consistent with evidence that hepatic insulin resistance predicts steatohepatitis and fibrosis independently of BMI, and with the observation that a substantial fraction of patients with MASLD are lean.

Mechanistically, chronic hyperglycaemia has been reported to promote hepatic de novo lipogenesis and to increase glycolytic flux, raising intracellular and circulating lactate. Beyond serving as a metabolic substrate, lactate is a precursor for lysine lactylation, an epigenetic

modification that has been linked to the transcriptional regulation of inflammatory and pro-fibrotic genes in experimental systems. Lactylation of histones and of non-histone proteins has been implicated in macrophage polarisation towards a pro-inflammatory phenotype [4], in hepatic stellate cell activation, and in impaired $CD8^+$ T-cell function within the liver microenvironment. The monotonic increase in serum lactate across glucose strata observed here, together with its correlation with parameters of adiposity and glycaemia, is consistent with this axis and provides a rationale for the exploratory transcriptomic analyses in Section 2.5. Interventional studies showing that improving glycaemic control reduces aminotransferases would further support a causal interpretation [27], although the present cross-sectional data cannot establish directionality.

Only 3.3% of participants with diagnosed diabetes had fasting glucose at or below the commonly used treatment target, and half of the entire cohort had fasting glucose in the diabetic range; 53 of these (20.7%) had not been labelled as having diabetes. Because aminotransferase elevation is frequently the presenting abnormality that brings these patients to medical attention, the liver clinic represents a practical opportunity for systematic glycaemic screening and intensification of treatment. In stratified analyses, the association between fasting glucose and ALT was strongest among participants in the lowest BMI tertile, with evidence of effect modification by BMI (P for interaction = 0.003). This finding suggests that dysglycaemia may be associated with greater relative ALT elevation even in individuals with lower BMI, who might otherwise be regarded as being at lower metabolic risk. Clinical risk assessment should therefore extend to individuals with lower BMI as well as to those with overweight or obesity, since lower adiposity does not exclude glucose-related liver injury. This was an exploratory subgroup finding without adjustment for multiple comparisons, and BMI does not capture visceral adiposity, ectopic fat deposition or sarcopenia, so it warrants cautious interpretation and confirmation in prospective studies.

The strengths of this study include a well-characterised cohort within the age range where fibrosis risk is clinically actionable, detailed metabolic phenotyping, hierarchical adjustment for adiposity and lipid variables, prespecified subgroup analyses, and internal assessment of additional explained variance. Several limitations must be acknowledged. First, the cross-sectional design precludes inference about temporality or causality; prospective follow-up with histological or elastographic endpoints is required. Second, liver injury was defined biochemically rather than histologically, and although FIB-4, NFS and APRI were calculated, none was validated against liver biopsy in this cohort. Third, the prevalence of diabetes was high relative to the general population of the same age, reflecting referral to a specialised metabolic liver clinic, and this may limit generalisability. Fourth, aminotransferase distributions were similar to those of younger referral populations; whether enzyme elevation in older adults follows the same distribution requires confirmation in prospective sampling. Fifth, single fasting glucose measurements are subject to acute variability, and HbA1c-based definitions may classify participants differently. Sixth, a uniform ALT upper limit of normal (40 U/L) was applied to both men and women; lower sex-specific thresholds have been proposed [28], so the uniform threshold may underestimate the prevalence of abnormal ALT, particularly in women. Seventh, FIB-4 incorporates AST and ALT, so the association between fasting glucose and elevated FIB-4 partly reflects mathematical

coupling with its aminotransferase components; elevated FIB-4 is therefore interpreted only as an exploratory risk category. Eighth, some adjustment variables (such as triglycerides and uric acid) may lie on the causal pathway between dysglycaemia and liver injury, and fully adjusted estimates should be read as adjusted associations rather than total effects. Finally, aetiological work-up was based on serology and history rather than systematic exclusion of all competing causes.

The transcriptomic findings add one nuance. Glycolytic and lactylation-related signatures were enriched in NASH and tracked serum ALT and histological activity, consistent with a glycolytic/lactate axis in injured liver. The insulin-signalling signature, however, was enriched in NASH but depleted in advanced fibrosis, a pattern consistent with metabolic dedifferentiation of hepatocytes during progression; accordingly, the module scores correlated with hepatic injury but showed no statistically significant association with systemic fasting glucose or HOMA-IR in the analysed dataset. These exploratory findings describe liver disease–associated transcriptional changes; whether systemic glycaemia drives this reprogramming cannot be determined from these data, and the lactylation-related gene sets reflect coordinated gene expression rather than directly measured protein or histone lactylation.

The apparent strengthening of the glucose coefficient after adjustment for adiposity warrants cautious interpretation. Fasting glucose was strongly correlated with BMI (Pearson $r = 0.84$), and BMI and waist circumference were strongly correlated with each other (variance inflation factors 11.9 and 19.3), so the fully adjusted model is subject to collinearity; the loss of statistical significance of the adiposity terms should therefore not be read as evidence that adiposity is unimportant in liver disease. The glucose estimate was nevertheless stable across adiposity adjustment strategies (GMR 1.087 with BMI alone, 1.086 with waist circumference alone and 1.090 with both), which supports the stability of the association while precluding strong claims that it is independent of adiposity.

In conclusion, in adults aged 45–65 years referred for elevated ALT, higher fasting plasma glucose was associated with higher ALT levels after adjustment for measured adiposity and other metabolic factors, and glycaemic control in this population was markedly suboptimal (median HbA1c 9.4% among participants with previously diagnosed diabetes). These findings support systematic glycaemic assessment in patients presenting with elevated ALT, but do not demonstrate causality or that glucose lowering reduces liver injury.

Tables

Table 1. Baseline characteristics of participants stratified by fasting glucose status (n = 511). P for trend from linear regression across glucose strata for continuous variables, the Cochran–Armitage test for binary variables, and the Cochran–Armitage trend test for ordinal steatosis grade.

Variable	Normal (<5.6) n=132	IFG (5.6 to <7.0) n=123	Diabetic range (7.0 to <10.0) n=111	Markedly elevated (≥10.0) n=145	p for trend
Age, years	55.5±5.8	55.0±5.8	54.2±5.9	55.3±5.7	0.715
Male, n (%)	67 (50.8)	78 (63.4)	66 (59.5)	90 (62.1)	0.110
Previously diagnosed diabetes, n (%)	0 (0.0)	7 (5.7)	58 (52.3)	145 (100.0)	<0.001
BMI, kg/m²	23.4±0.9	25.6±1.0	26.3±1.7	28.2±1.6	<0.001
Waist circumference, cm	80.0±4.9	86.3±6.0	87.7±7.7	93.1±7.3	<0.001
Systolic BP, mmHg	123.6±20.6	127.6±20.4	129.3±18.9	133.9±20.1	<0.001
ALT, U/L, median (IQR)	128 (78–181)	132 (82–190)	167 (92–232)	192 (140–247)	<0.001
AST, U/L, median (IQR)	46 (30–86)	51 (33–81)	65 (42–111)	95 (70–135)	<0.001
GGT, U/L, median (IQR)	46 (28–58)	41 (26–55)	41 (23–56)	45 (27–57)	0.671
Platelet count, ×10⁹/L	207.9±39.8	207.3±40.4	208.7±42.9	206.1±45.3	0.933
Albumin, g/L	44.0±3.0	44.5±3.3	44.2±3.2	43.8±3.1	0.659
Triglycerides, mmol/L	2.0±0.8	2.7±0.8	2.6±0.8	3.0±0.6	<0.001
HbA1c, %	4.91±0.42	5.54±0.64	6.68±0.76	10.53±1.89	<0.001
Serum lactate, mmol/L	1.20±0.29	1.29±0.30	1.38±0.32	1.77±0.35	<0.001
FIB-4, median (IQR)	1.35 (0.90–1.98)	1.44 (0.94–1.94)	1.43 (1.00–2.32)	1.86 (1.30–2.70)	<0.001
FIB-4 ≥2.67, n (%)	10 (7.6)	11 (8.9)	21 (18.9)	38 (26.2)	<0.001
Steatosis grade 0/1/2/3, n	80/41/11/0	21/62/30/10	20/37/36/18	5/27/43/70	<0.001

Table 2. Association between fasting glucose and categorical liver outcomes

Outcome	Prevalence by glucose stratum (normal / IFG / 7.0 to <10.0 / ≥10)	Adjusted OR per +1 mmol/L (95% CI)	p
ALT ≥3×ULN (120 U/L)	53.8% / 55.3% / 64.0% / 83.4%	1.211 (1.099–1.335)	1.1×10^{-4}
ALT ≥5×ULN (200 U/L)*	17.4% / 17.9% / 40.5% / 46.9%	1.175 (1.067–1.294)	1.0×10^{-3}
FIB-4 ≥2.67†	7.6% / 8.9% / 18.9% / 26.2%	1.274 (1.103–1.471)	9.6×10^{-4}

Odds ratios are per 1 mmol/L increment in fasting glucose, adjusted for age, sex, BMI, waist circumference, triglycerides, total cholesterol and uric acid (Model 3). *Exploratory outcome. †Exploratory risk category; FIB-4 incorporates aminotransferase values and participants were enrolled on the basis of elevated ALT, so elevated FIB-4 should not be interpreted as confirmed structural fibrosis.

Table 3. Multivariable linear regression for log-transformed ALT

Variable	Model 1: ALT GMR (95% CI)	Model 2: ALT GMR (95% CI)	Model 3: ALT GMR (95% CI)	Model 3 P
Fasting plasma glucose, per 1 mmol/L increase	1.050 (1.037–1.063)	1.051 (1.038–1.065)	1.090 (1.062–1.118)	2.4×10^{-10}
Male sex	—	0.908 (0.814–1.014)	1.053 (0.773–1.433)	0.745
Age (per year)	—	0.999 (0.990–1.009)	0.999 (0.989–1.008)	0.751
BMI (per kg/m²)	—	—	0.966 (0.890–1.048)	0.405
Waist circumference (per cm)	—	—	0.984 (0.956–1.012)	0.260
Triglycerides (per mmol/L)	—	—	0.951 (0.885–1.023)	0.176
Total cholesterol (per mmol/L)	—	—	1.009 (0.881–1.157)	0.892
Uric acid (per μmol/L)	—	—	1.001 (0.999–1.002)	0.327

Model 1 unadjusted; Model 2 adjusted for age and sex; Model 3 additionally adjusted for BMI, waist circumference, triglycerides, total cholesterol and uric acid. Estimates are geometric mean ratios (GMR) of ALT per unit increase in each variable from linear models on log-transformed ALT. Stratum-specific GMRs relative to the normal-glucose group (the categorical display) are provided in Supplementary Table S1.

Table 4. Glycaemic control and clinical management gap

FPG, fasting plasma glucose. A single fasting glucose measurement does not capture long-term glycaemic control; HbA1c results are therefore also reported. Cohort-wide, 177 participants used antihyperglycaemic medication, of whom 172 had previously diagnosed diabetes and 5 had no recorded diagnosis.

Parameter	Value
Participants with diabetes, n	210
FPG <7.0 mmol/L at the study visit, n (%)	7 (3.3)
FPG ≥7.0 mmol/L, n (%)	203 (96.7)
Whole cohort with FPG ≥7.0 mmol/L, n (%)	256 (50.1)
FPG ≥7.0 mmol/L but not labelled as diabetes, n	53
Median ALT, diabetes vs no diabetes (U/L)	192 vs 129
Antidiabetic medication use among diabetes, n (%)	172 (81.9)
HbA1c among participants with previously diagnosed diabetes (n = 210), %, median (IQR)	9.4 (7.5–11.1)
HbA1c ≥7.0% among participants with previously diagnosed diabetes, n/N (%)	174/210 (82.9)

Table 5. Supplementary clinical variables stratified by fasting glucose status

Characteristic	<5.6 (n=132)	5.6 to <7.0 (n=123)	7.0 to <10.0 (n=111)	≥10.0 (n=145)
HbA1c, %, median (IQR)	4.6 (4.6–5.1)	5.6 (5.0–6.0)	6.7 (6.2–7.2)	10.2 (9.3–11.9)
Diabetes duration, y, median (IQR)*	—	8.0 (7.3–10.3)	10.8 (8.1–12.9)	10.4 (8.2–13.3)
Hepatic steatosis on ultrasound, n/N (%)	52/132 (39.4)	102/123 (82.9)	91/111 (82.0)	140/145 (96.6)
Moderate-to-severe steatosis (grade 2–3), n/N (%)	11/132 (8.3)	40/123 (32.5)	54/111 (48.6)	113/145 (77.9)
Liver stiffness, kPa, median (IQR)	5.2 (4.4–6.1)	5.3 (4.5–6.0)	5.2 (4.5–6.0)	5.7 (4.8–6.5)
Liver stiffness ≥8 kPa, n/N (%)	0/132 (0)	4/123 (3.3)	4/111 (3.6)	8/145 (5.5)
CAP, dB/m, median (IQR)	247 (230–267)	271 (254–287)	273 (254–286)	294 (276–312)
Any antihyperglycaemic medication, n/N (%)	2/132 (1.5)	10/123 (8.1)	48/111 (43.2)	117/145 (80.7)
HOMA-IR, median (IQR)	1.9 (1.5–2.4)	3.0 (2.3–3.5)	4.2 (3.4–5.1)	9.2 (7.3–12.9)

*HbA1c, glycated haemoglobin; CAP, controlled attenuation parameter; HOMA-IR, homeostatic model assessment of insulin resistance; IQR, interquartile range. All variables were available for all 511 participants (no missing data); n/N uses stratum denominators. *Diabetes duration among participants with previously diagnosed diabetes (n = 7, 58 and 145 in the three higher strata). Antihyperglycaemic medication counts are cohort-wide (177 users, of whom 172 had previously diagnosed diabetes; see Table 4).*

Supplementary Table S1. Stratum-specific geometric mean ratios of ALT relative to the normal-glucose group

Fasting-glucose stratum	Model 1: GMR (95% CI)	Model 2: GMR (95% CI)	Model 3: GMR (95% CI)	Model 3 P
Normal (<5.6 mmol/L)	1 (reference)	1 (reference)	1 (reference)	—
IFG (5.6 to <7.0)	1.06 (0.91–1.23)	1.07 (0.92–1.24)	1.28 (1.07–1.52)	5.8×10^{-3}
Diabetic range (7.0 to <10.0)	1.31 (1.13–1.53)	1.32 (1.13–1.54)	1.66 (1.36–2.02)	7.5×10^{-7}
Markedly elevated (≥10.0)	1.80 (1.56–2.08)	1.82 (1.57–2.10)	2.68 (2.06–3.47)	4.5×10^{-13}

GMR, geometric mean ratio of ALT from linear models on log-transformed ALT. Model 1 unadjusted; Model 2 adjusted for age and sex; Model 3 additionally adjusted for BMI, waist circumference, triglycerides, total cholesterol and uric acid.

Supplementary Table S2. Custom gene sets used in the transcriptomic analyses

Gene set	n genes	Member genes (HGNC symbols)
Lactylation machinery	90	EP300, CREBBP, KAT2A, KAT2B, KAT5, KAT6A, KAT6B, KAT7, KAT8, KAT14, HDAC1, HDAC2, HDAC3, HDAC6, HDAC8, SIRT1, SIRT2, SIRT3, SIRT5, SIRT6, SIRT7, AARS1, AARS2, ELP3, NAA10, NAA15, NAA50, KANSL1, KANSL2, KANSL3, LDHA, LDHB, LDHC, LDHD, SLC16A1, SLC16A3, SLC16A7, SLC16A8, SLC2A1, SLC2A2, SLC2A3, SLC2A4, HK1, HK2, HK3, GCK, PFKL, PFKM, PFKP, PFKFB1, PFKFB2, PFKFB3, PFKFB4, ALDOA, ALDOB, ALDOC, TPI1, GAPDH, PGK1, PGAM1, PGAM2, ENO1, ENO2, ENO3, PKM, PKLR, HIF1A, ARNT, EPAS1, VHL, PDK1, PDK2, PDK3, PDHA1, PDHB, DLAT, MPC1, MPC2, ACSS1, ACSS2, ACACA, ACACB, FASN, SCD, GYS1, GYS2, PYGL, PYGM, NNMT, ATP6AP1
Glycolysis/lactate metabolism	67	HK1, HK2, HK3, GCK, GPI, PFKL, PFKM, PFKP, PFKFB1, PFKFB2, PFKFB3, PFKFB4, ALDOA, ALDOB, ALDOC, TPI1, GAPDH, PGK1, PGAM1, PGAM2, ENO1, ENO2, ENO3, PKM, PKLR, LDHA, LDHB, LDHC, LDHD, SLC16A1, SLC16A3, SLC16A7, SLC16A8, SLC2A1, SLC2A2, SLC2A3, SLC2A4, SLC2A5, SLC2A6, HIF1A, ARNT, EPAS1, VHL, PDK1, PDK2, PDK3, PDK4, PDHA1, PDHB, DLAT, DLD, MPC1, MPC2, PC, PCK1, PCK2, FBP1, G6PC, GYS1, GYS2, PYGL, PYGM, UGP2, NNMT, ACSS1, ACSS2, ACLY
Insulin signalling	76	INS, IGF1, IGF2, INSR, IGF1R, IRS1, IRS2, IRS4, SHC1, GRB2, SOS1, HRAS, RAF1, MAP2K1, MAP2K2, MAPK1, MAPK3, PIK3CA, PIK3CB, PIK3CD, PIK3CG, PIK3R1, PIK3R2, PIK3R3, AKT1, AKT2, AKT3, MTOR, RPTOR, RICTOR, TSC1, TSC2, RHEB, RPS6KB1, RPS6KB2, EIF4EBP1, FOXO1, FOXO3, FOXO4, GSK3A, GSK3B, SLC2A4, TBC1D1, TBC1D4, PTPN1, PTPRF, INPP5E, INPP5K, PPARGC1A, PRKAA1, PRKAA2, PRKAB1, PRKAB2, PRKAG1, PRKAG2, PRKAG3, PYGL, PYGM, GYS1, GYS2, PCK1, PCK2, FBP1, G6PC, PPP1R3A, PPP1R3B, PPP1R3C, SLC2A2, SLC27A2, GCK, GK, HNF4A, PPARA, CEBPA, INSIG1, SREBF1

Gene sets were assembled from curated pathway members (lactylation writers/erasers/readers and substrate-supply enzymes; glycolytic and lactate-production/transport genes; KEGG hsa04910-homologous insulin-signalling members) and used both in preranked GSEA and as single-sample module scores.

Supplementary Table S3. Spearman correlation matrix of continuous covariates (n = 511)

Variable	FPG	HbA1c	Age	BMI	Waist	TG	TC	UA	Lactate	ALT
FPG, mmol/L	1.00									
HbA1c, %	0.92	1.00								
Age, y	-0.04	-0.03	1.00							
BMI, kg/m²	0.86	0.77	-0.04	1.00						
Waist, cm	0.63	0.56	-0.06	0.79	1.00					
TG, mmol/L	0.57	0.49	-0.01	0.63	0.50	1.00				
TC, mmol/L	0.63	0.58	0.02	0.48	0.32	0.32	1.00			
UA, μmol/L	0.17	0.13	-0.03	0.23	0.60	0.19	0.06	1.00		
Lactate, mmol/L	0.59	0.56	0.05	0.54	0.40	0.38	0.34	0.07	1.00	
ALT, U/L	0.33	0.32	-0.01	0.19	0.11	0.10	0.18	0.02	0.35	1.00

Lower triangle shown; Spearman coefficients. All variables were complete for the 511 participants (no missing data). The BMI–waist correlation was ρ = 0.79 (Pearson r = 0.81); variance inflation factors in the fully adjusted model were 11.9 (BMI) and 19.3 (waist circumference).

Figure legends

Figure 1. Study flow and baseline distribution. (a) Participant flow (n = 511 after exclusions). (b) Age distribution (median 55, IQR 51–59). (c) Fasting plasma glucose distribution coloured by glycaemic stratum (<5.6, 5.6 to <7.0, 7.0 to <10.0, ≥10.0 mmol/L; n = 132/123/111/145). (d) ALT distribution with 1×, 3× and 5× ULN thresholds. (e) ALT by glycaemic stratum (log scale; boxes, IQR; central line, median). (f) FIB-4 distribution with 1.3 and 2.67 risk thresholds.

Figure 2. Restricted cubic spline dose–response between fasting plasma glucose and liver injury. (a) Continuous ALT expressed as fold change relative to 5.6 mmol/L (linear model). (b, c) Odds ratios for ALT ≥3×ULN and ALT ≥5×ULN (logistic models; log scale). Curves are adjusted for sex, age, BMI, waist circumference, triglycerides, total cholesterol and uric acid; shaded bands, 95% confidence intervals; white points, stratum-specific estimates; rug marks, observed glucose values; dashed line, 7.0 mmol/L. P-overall and P-nonlinear from likelihood-ratio tests.

Figure 3. Subgroup analyses of the fasting-glucose–ALT association. Adjusted geometric mean ratios (GMR) of ALT per +1 mmol/L fasting plasma glucose within prespecified subgroups, each model adjusted for sex, age, BMI, waist circumference, triglycerides, total cholesterol and uric acid; interaction tested with glucose × subgroup product terms. The diabetes subgroup is defined by previously diagnosed diabetes; because only 7 of 210 participants with diabetes had fasting glucose below 7.0 mmol/L at the study visit, the within-stratum exposure range is restricted and the interaction test is not reported for this subgroup.

Figure 4. Incremental value of adding glucose strata to a clinical model. (a, b) ROC curves for ALT ≥3×ULN and FIB-4 ≥2.67 (clinical model vs clinical model + glucose strata). (c) ΔAUC with bootstrap 95% confidence intervals, DeLong P values, ΔAIC and likelihood-ratio (LR) tests. FIB-4 ≥2.67 is an exploratory outcome; reclassification metrics and decision-curve analysis are not reported given the cross-sectional design and the absence of a defined clinical decision scenario.

Figure 5. Gene-set enrichment across three public MASLD liver cohorts. (a) Normalised enrichment score (NES) bubble matrix for ten gene sets across five analyses: two categorical NASH contrasts (GSE48452, GSE89632), two continuous GSE135251 contrasts (vs NAFLD activity score and vs fibrosis stage) and binary advanced fibrosis (F3–4 vs F0–1). Bubble size, −log10(FDR); orange/blue, positive/negative NES; faded, FDR ≥0.05; dagger, nominal P <0.05. (b) Running-enrichment plot for KEGG glycolysis/gluconeogenesis in GSE48452 (NES = +2.08, FDR = 0.001). (c) Running-enrichment plot for the custom insulin-signalling set in GSE89632 (NES = +1.52, FDR = 0.014).

Figure 6. Immune remodelling and module–clinical trait associations. (a) Marker-based cell-type module scores by fibrosis stage in GSE135251 (row z-score; n per stage shown). (b) Spearman correlation of each cell-type score with fibrosis stage. (c) Insulin-signalling and lactylation module scores vs serum ALT (log scale; GSE89632). (d) Module scores vs metabolic traits (fasting glucose, HOMA-IR, NAFLD activity score, fibrosis stage), Spearman ρ with Fisher-z 95% confidence intervals.

Declarations

Ethics approval and consent to participate.

Written informed consent was obtained from all participants in this study. Given the retrospective design of the study, ethical review was waived by the Science and Technology Ethics Committee of The Second Hospital of Nanjing.All procedures involving human participants, human data or human specimens in this report were performed in accordance with relevant guidelines and regulations.

Availability of data and materials.

The de-identified participant-level data analysed during the current study are available from the corresponding author on reasonable request, subject to institutional data-sharing policies and ethics-committee requirements; individual data will not be shared publicly to protect participant

privacy. The public transcriptomic datasets analysed are available in the Gene Expression Omnibus under accession numbers GSE48452, GSE89632 and GSE135251.

Funding Declaration.

The authors declare that no financial support was obtained for this research.

Conflict of Interest Statement.

The authors declare that there is no conflict of interest.

Author contributions.

These authors contributed equally to this work.

Reporting guideline.

This study is reported in accordance with the STROBE statement for cross-sectional studies; the completed checklist is provided as Supplementary Material.

Consent for publication.

Not applicable.

References

1. Younossi ZM, Koenig AB, Abdelatif D, Fazel Y, Henry L, Wymer M. Global epidemiology of nonalcoholic fatty liver disease—meta-analytic assessment of prevalence, incidence, and outcomes. Hepatology. 2016;64(1):73–84.

2. Rinella ME, Lazarus JV, Ratziu V, et al. A multisociety Delphi consensus statement on new fatty liver disease nomenclature. Hepatology. 2023;78(6):1966–1986.

3. Samuel VT, Shulman GI. Mechanisms for insulin resistance: common threads and missing links. Cell. 2012;148(5):852–871.

4. Zhang D, Tang Z, Huang H, et al. Metabolic regulation of gene expression by histone lactylation. Nature. 2019;574(7779):575–580.

5. McPherson S, Hardy T, Dufour JF, et al. Age as a confounding factor for the accurate non-invasive diagnosis of advanced NAFLD fibrosis. Am J Gastroenterol. 2017;112(5):740–751.

6. Hernaez R, Lazo M, Bonekamp S, et al. Diagnostic accuracy and reliability of ultrasonography for the detection of fatty liver: a meta-analysis. Hepatology. 2011;54(3):1082–1090.

7. Eddowes PJ, Sasso M, Allison M, et al. Accuracy of FibroScan controlled attenuation parameter and liver stiffness measurement in assessing steatosis and fibrosis in patients with nonalcoholic fatty liver disease. Gastroenterology. 2019;156(6):1717–1730.

8. de Franchis R, Bosch J, Garcia-Tsao G, Reiberger T, Ripoll C; Baveno VII Faculty. Baveno VII—renewing consensus in portal hypertension. J Hepatol. 2022;76(4):959–974.

9. Sterling RK, Lissen E, Clumeck N, et al. Development of a simple noninvasive index to predict significant fibrosis in patients with HIV/HCV coinfection. Hepatology. 2006;43(6):1317–1325.

10. American Diabetes Association Professional Practice Committee. 2. Diagnosis and classification of diabetes: Standards of Care in Diabetes—2025. Diabetes Care. 2025;48(Suppl 1):S27–S49.

11. Angulo P, Hui JM, Marchesini G, et al. The NAFLD fibrosis score: a noninvasive system that identifies liver fibrosis in patients with NAFLD. Hepatology. 2007;45(4):846–854.

12. Wai CT, Greenson JK, Fontana RJ, et al. A simple noninvasive index can predict both significant fibrosis and cirrhosis in patients with chronic hepatitis C. Hepatology. 2003;38(2):518–526.

13. Harrell FE Jr. Regression Modeling Strategies: With Applications to Linear Models, Logistic and Ordinal Regression, and Survival Analysis. 2nd ed. Cham: Springer; 2015.

14. DeLong ER, DeLong DM, Clarke-Pearson DL. Comparing the areas under two or more correlated receiver operating characteristic curves: a nonparametric approach. Biometrics. 1988;44(3):837–845.

15. Benjamini Y, Hochberg Y. Controlling the false discovery rate: a practical and powerful approach to multiple testing. J R Stat Soc Series B Stat Methodol. 1995;57(1):289–300.

16. von Elm E, Altman DG, Egger M, Pocock SJ, Gøtzsche PC, Vandenbroucke JP; STROBE Initiative. The Strengthening the Reporting of Observational Studies in Epidemiology (STROBE) statement: guidelines for reporting observational studies. Lancet. 2007;370(9596):1453–1457.

17. Ahrens M, Ammerpohl O, von Schönfels W, et al. DNA methylation analysis in nonalcoholic fatty liver disease suggests distinct disease-specific and remodeling signatures after bariatric surgery. Cell Metab. 2013;18(2):296–302.

18. Arendt BM, Comelli EM, Ma DWL, et al. Altered hepatic gene expression in nonalcoholic fatty liver disease is associated with lower hepatic n-3 and n-6 polyunsaturated fatty acids. Hepatology. 2015;61(5):1565–1578.

19. Govaere O, Cockell S, Tiniakos D, et al. Transcriptomic profiling across the nonalcoholic fatty liver disease spectrum reveals gene signatures for steatohepatitis and fibrosis. Sci Transl Med. 2020;12(572):eaba4448.

20. Subramanian A, Tamayo P, Mootha VK, et al. Gene set enrichment analysis: a knowledge-based approach for interpreting genome-wide expression profiles. Proc Natl Acad Sci U S A. 2005;102(43):15545–15550.

21. Liberzon A, Birger C, Thorvaldsdóttir H, Ghandi M, Mesirov JP, Tamayo P. The Molecular Signatures Database (MSigDB) hallmark gene set collection. Cell Syst. 2015;1(6):417–425.

22. Kanehisa M, Goto S. KEGG: Kyoto encyclopedia of genes and genomes. Nucleic Acids Res. 2000;28(1):27–30.

23. Jassal B, Matthews L, Viteri G, et al. The reactome pathway knowledgebase. Nucleic Acids Res. 2020;48(D1):D498–D503.

24. Bindea G, Mlecnik B, Tosolini M, et al. Spatiotemporal dynamics of intratumoral immune cells reveal the immune landscape in human cancer. Immunity. 2013;39(4):782–795.

25. Barbie DA, Tamayo P, Boehm JS, et al. Systematic RNA interference reveals that oncogenic KRAS-driven cancers require TBK1. Nature. 2009;462(7269):108–112.

26. Fang Z, Liu X, Peltz G. GSEApy: a comprehensive package for performing gene set enrichment analysis in Python. Bioinformatics. 2023;39(1):btac757.

27. Newsome PN, Buchholtz K, Cusi K, et al. A placebo-controlled trial of subcutaneous semaglutide in nonalcoholic steatohepatitis. N Engl J Med. 2021;384(12):1113–1124.

28. Prati D, Taioli E, Zanella A, et al. Updated definitions of healthy ranges for serum alanine aminotransferase levels. Ann Intern Med. 2002;137(1):1–10.

Figure 1

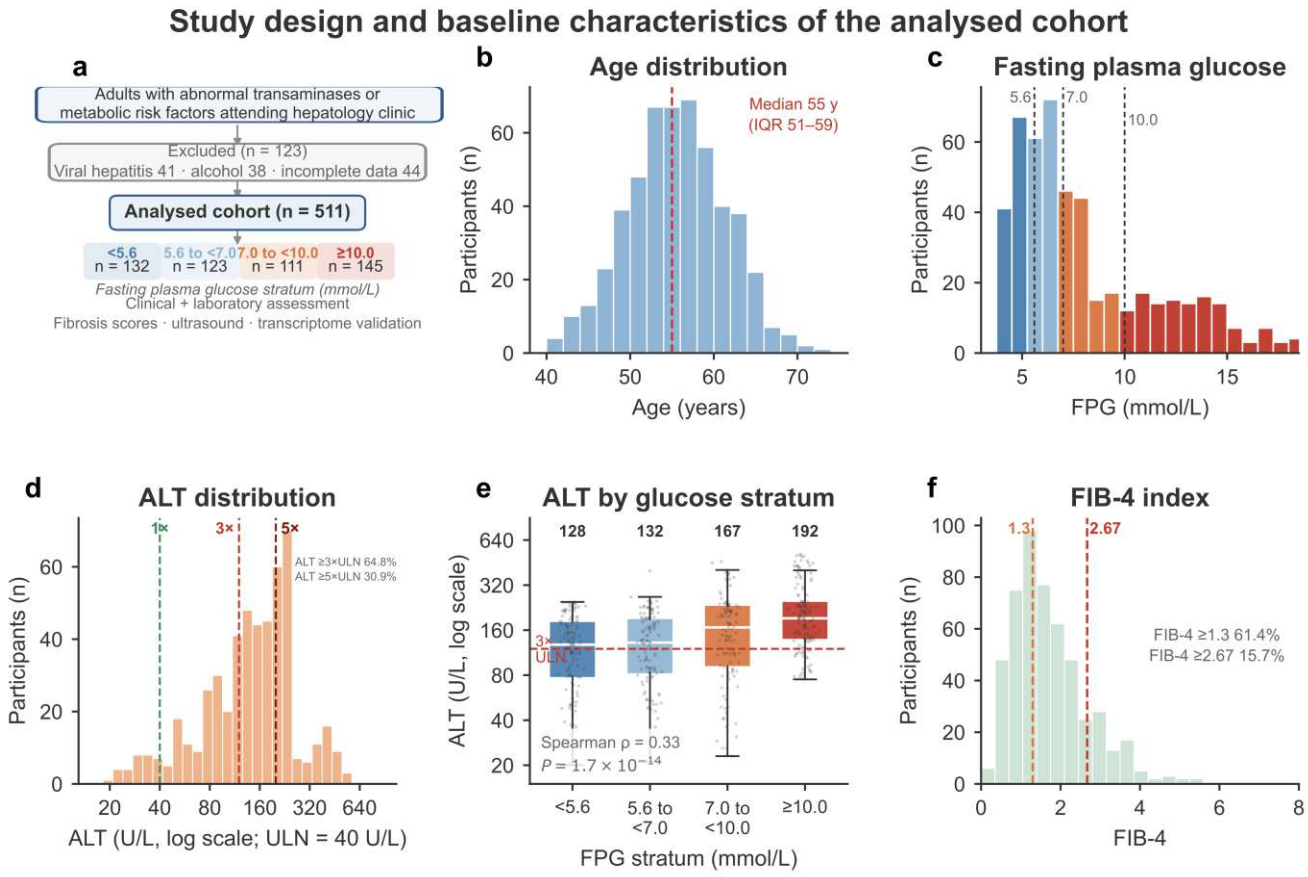


Figure 1. Study flow and baseline distribution. (a) Participant flow (n = 511 after exclusions). (b) Age distribution (median 55, IQR 51–59). (c) Fasting plasma glucose distribution coloured by glycaemic stratum (<5.6, 5.6 to <7.0, 7.0 to <10.0, ≥10.0 mmol/L; n = 132/123/111/145). (d) ALT distribution with 1×, 3× and 5× ULN thresholds. (e) ALT by glycaemic stratum (log scale; boxes, IQR; central line, median). (f) FIB-4 distribution with 1.3 and 2.67 risk thresholds.

Figure 2

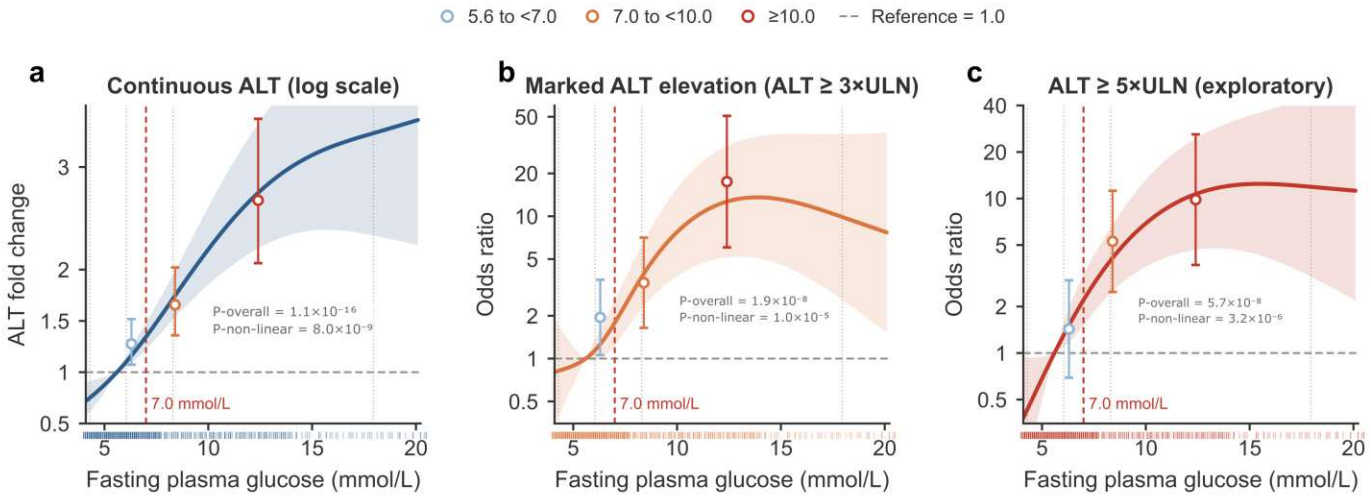


Figure 2. Restricted cubic spline dose–response between fasting plasma glucose and liver injury. (a) Continuous ALT expressed as fold change relative to 5.6 mmol/L (linear model). (b, c) Odds ratios for ALT ≥3×ULN and ALT ≥5×ULN (logistic models; log scale). Curves are adjusted for sex, age, BMI, waist circumference, triglycerides, total cholesterol and uric acid; shaded bands, 95% confidence intervals; white points, stratum-specific estimates; rug marks, observed glucose values; dashed line, 7.0 mmol/L. P-overall and P-nonlinear from likelihood-ratio tests.

Figure 3

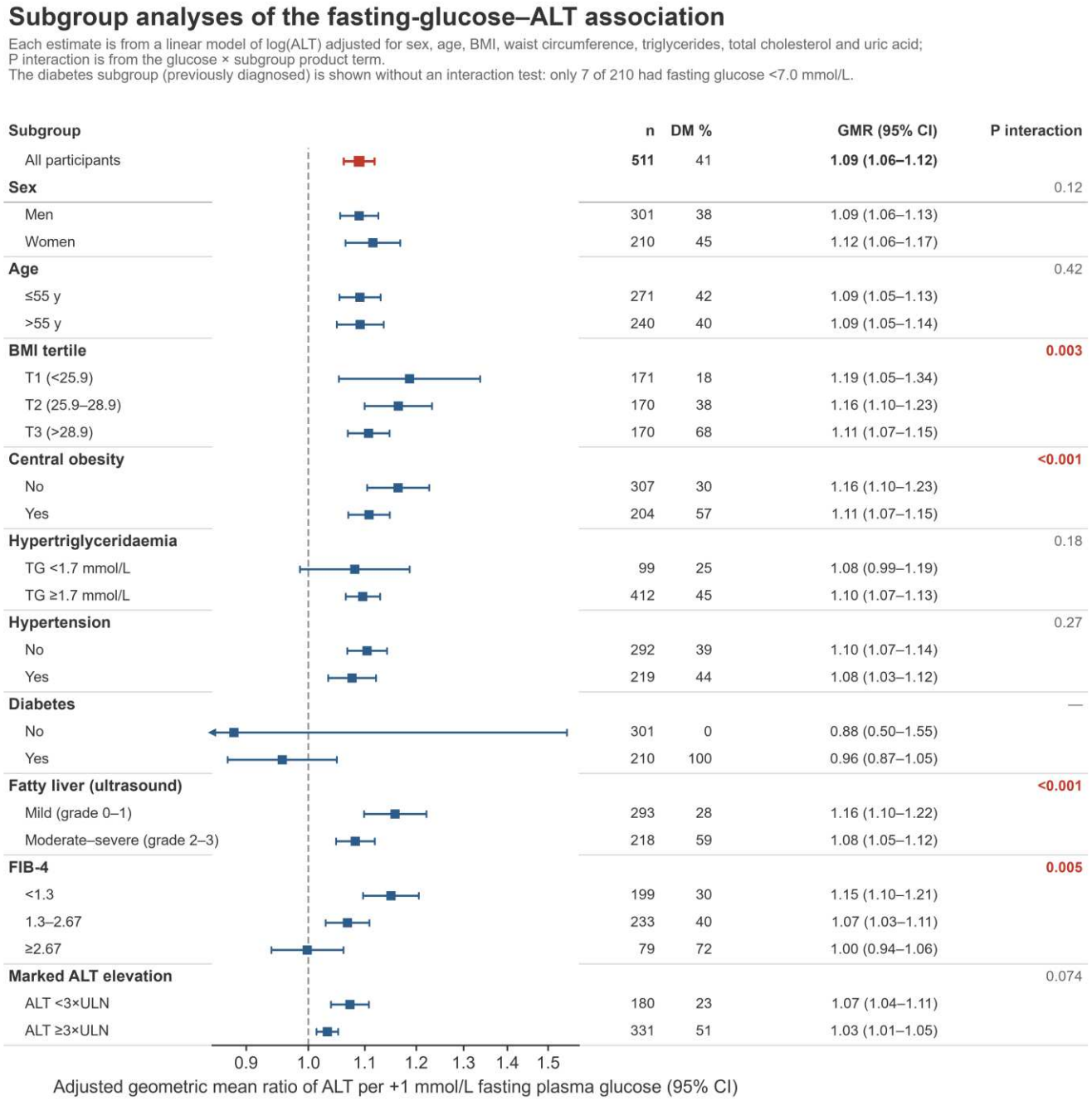


Figure 3. Subgroup analyses of the fasting-glucose–ALT association. Adjusted geometric mean ratios (GMR) of ALT per +1 mmol/L fasting plasma glucose within prespecified subgroups, each model adjusted for sex, age, BMI, waist circumference, triglycerides, total cholesterol and uric acid; interaction tested with glucose × subgroup product terms. The diabetes subgroup is defined by previously diagnosed diabetes; because only 7 of 210 participants with diabetes had fasting

glucose below 7.0 mmol/L at the study visit, the within-stratum exposure range is restricted and the interaction test is not reported for this subgroup.

Figure 4

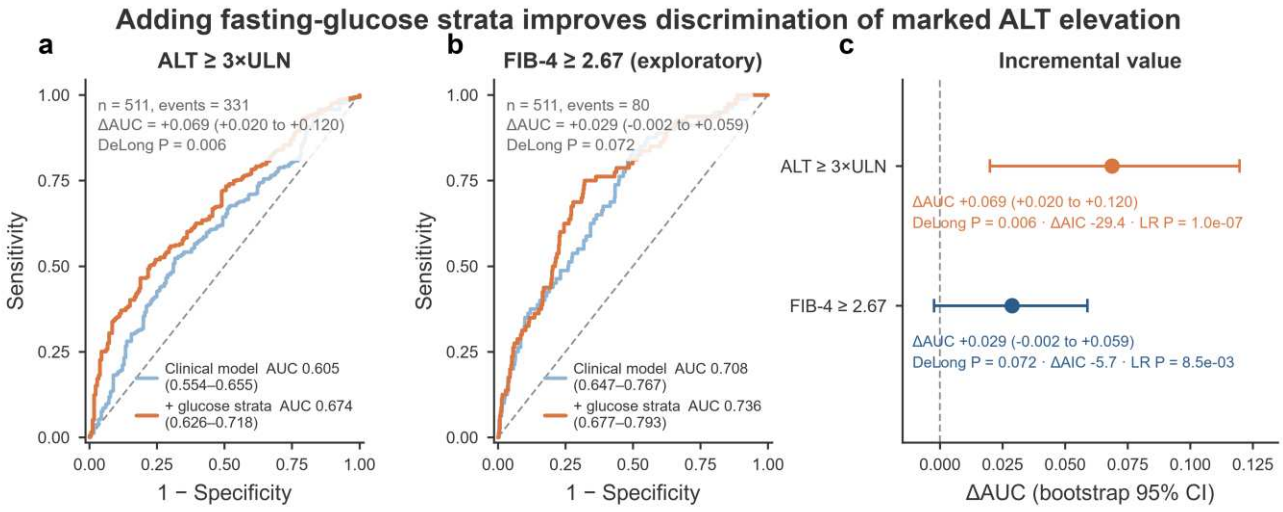


Figure 4. Incremental value of adding glucose strata to a clinical model. (a, b) ROC curves for ALT ≥3×ULN and FIB-4 ≥2.67 (clinical model vs clinical model + glucose strata). (c) ΔAUC with bootstrap 95% confidence intervals, DeLong P values, ΔAIC and likelihood-ratio (LR) tests. FIB-4 ≥2.67 is an exploratory outcome; reclassification metrics and decision-curve analysis are not reported given the cross-sectional design and the absence of a defined clinical decision scenario.

Figure 5

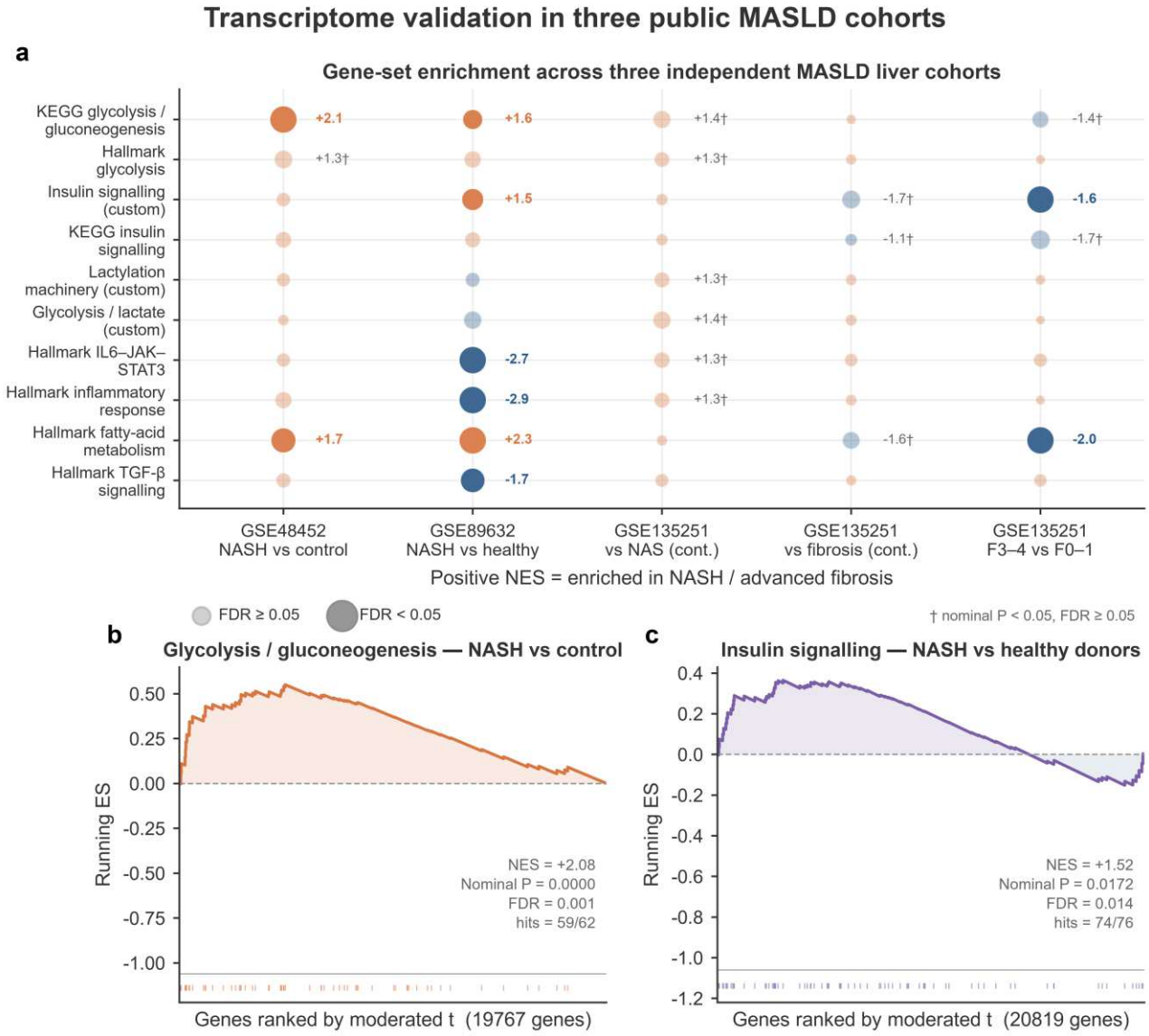


Figure 5. Gene-set enrichment across three public MASLD liver cohorts. (a) Normalised enrichment score (NES) bubble matrix for ten gene sets across five analyses: two categorical NASH contrasts (GSE48452, GSE89632), two continuous GSE135251 contrasts (vs NAFLD activity score and vs fibrosis stage) and binary advanced fibrosis (F3–4 vs F0–1). Bubble size, −log10(FDR); orange/blue, positive/negative NES; faded, FDR ≥0.05; dagger, nominal P <0.05. (b) Running-enrichment plot for KEGG glycolysis/gluconeogenesis in GSE48452 (NES = +2.08, FDR = 0.001). (c) Running-enrichment plot for the custom insulin-signalling set in GSE89632 (NES = +1.52, FDR = 0.014).

Figure 6

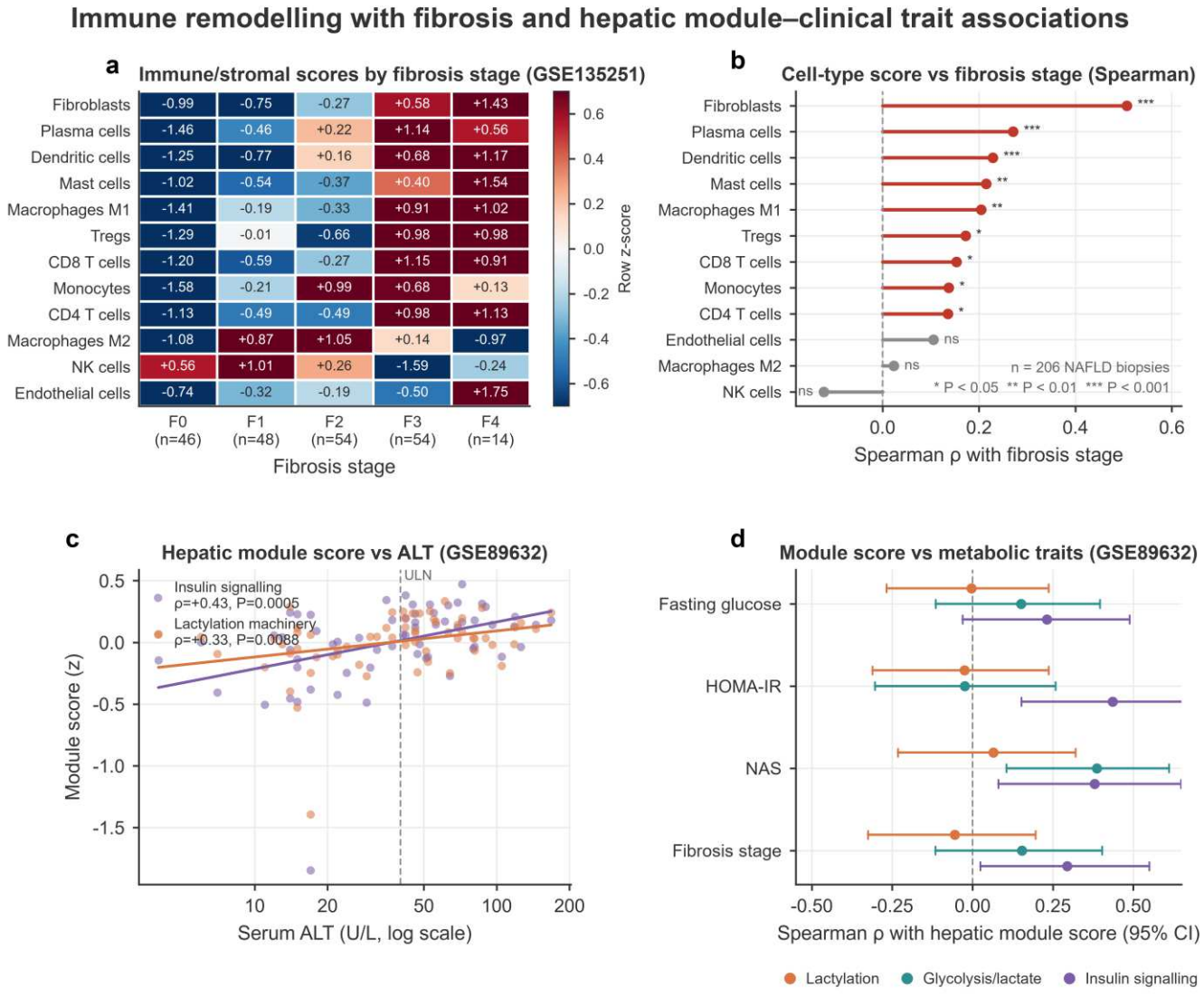


Figure 6. Immune remodelling and module–clinical trait associations. (a) Marker-based cell-type module scores by fibrosis stage in GSE135251 (row z-score; n per stage shown). (b) Spearman correlation of each cell-type score with fibrosis stage. (c) Insulin-signalling and lactylation module scores vs serum ALT (log scale; GSE89632). (d) Module scores vs metabolic traits (fasting glucose, HOMA-IR, NAFLD activity score, fibrosis stage), Spearman ρ with Fisher-z 95% confidence intervals.